Polymer 51 (2010) 1779–1785

Contents lists available at ScienceDirect

Polymer

journal homepage: www.elsevier.com/locate/polymer

Optimization of thermal remendability of epoxy via blending

Qiao Tian [a,b], Min Zhi Rong [b], Ming Qiu Zhang [b,*], Yan Chao Yuan [a,b]

[a] Key Laboratory for Polymeric Composite and Functional Materials of Ministry of Education, DSAPM Lab, School of Chemistry and Chemical Engineering, Zhongshan University, Guangzhou 510275, PR China
[b] Materials Science Institute, Zhongshan University, Guangzhou 510275, PR China

ARTICLE INFO

Article history:
Received 7 December 2009
Received in revised form
21 January 2010
Accepted 3 February 2010
Available online 10 February 2010

Keywords:
Epoxy
Thermal reversibility
Diels–Alder bonds

ABSTRACT

To prepare epoxy materials with improved thermal remendability, two types of epoxy resins (*N*,*N*-diglycidyl-furfurylamine (DGFA) and furfuryl glycidyl ether (FGE)), which were synthesized in the authors' lab and contained different proportions of furan and epoxide groups, were blended and cured by anhydride and maleimide. Like the cured version of either DGFA or FGE alone, the cured blends of DGFA and FGE have also acquired thermal reversibility due to the Diels–Alder (DA) bonds from the reaction between furan and maleimide groups. The addition of FGE into the blends increased the DA bonds density as a result of the higher furan concentration in FGE. Accordingly, remendability originating from successive retro-DA and DA reactions was obviously improved. On the other hand, the crosslinked epoxy networks generated by the reaction between epoxide and anhydride groups were strong enough to provide the blends with acceptable mechanical performance.

1. Introduction

During manufacturing and service, polymers and polymer composites would easily generate internal microcracks. Development and coalescence of these defects would bring about catastrophic failure of the materials and then reduce their lifetimes. Therefore, synthesis of polymers being able to remove damages and recover properties under the stimulus of certain mechanism would be a reasonable solution [1,2].

Recent explorations in this area have shown the prospects of thermally remendable macromolecules. For example, Wudl and coworkers produced highly crosslinked polymeric materials with multi-furan and multi-maleimide via Diels–Alder (DA) reaction [3,4]. At temperatures above 120 °C, the intermonomer linkages disconnect (corresponding to retro-DA reaction) but then reconnect upon cooling (i.e. DA reaction). This process is fully reversible and can be used to restore fractured parts of the polymers. In principle, an infinite of crack healing is available without the aid of additional catalysts, monomers and special surface treatment. Similarly, Liu et al. prepared a thermally remendable and removable crosslinked polymer through DA reactions between multifunctional furan and maleimide monomers by using epoxy compounds as precursors [5]. In a subsequent work, they reported thermally reversible crosslinked polyamides from maleimide-containing polyamides and a tri-functional furan compound [6].

Having been inspired by the above concept, we made a thermally remendable epoxy resin, *N*,*N*-diglycidyl-furfurylamine (DGFA) (Scheme 1(a)) [7]. It contains both furan and epoxide groups. When the resin is cured by anhydride and maleimide, two types of intermonomer linkage are generated: thermally reversible DA bonds from the reaction between furan and maleimide groups (Scheme 2), and thermally stable bonds from the reaction between epoxide and anhydride groups. The DA bonds offer crack repair effect based on successive retro-DA and DA reactions induced chain reconnection, while epoxy networks act as the fixing phase. Such a specific molecular structure enables rehabilitation below glass transition temperature of the material, so that distortion during crack healing can be avoided.

Due to the relatively less amount of furan in the molecules, however, the healing efficiency of cured DGFA is not satisfactory enough (see the result hereinafter). Therefore, another epoxy monomer, furfuryl glycidyl ether (FGE, Scheme 1(b)), was synthesized in the authors' lab [8]. It has a similar structure like DGFA, while the fraction of furan is higher. Almost full recovery of thermal reversibility of DA bonds in cured FGE was observed in the course of repeated heating and cooling. Nevertheless, apart from the above positive effect, it is worth noting that only one epoxide group is present in each FGE molecule. Contribution of epoxy bonds to the cured FGE is thus limited, which is disadvantageous to the mechanical performance. Additionally, the retro-DA temperature of

* Corresponding author. Fax: +86 20 84114008.
E-mail address: ceszmq@mail.sysu.edu.cn (M.Q. Zhang).

0032-3861/$ – see front matter © 2010 Elsevier Ltd. All rights reserved.
doi:10.1016/j.polymer.2010.02.004

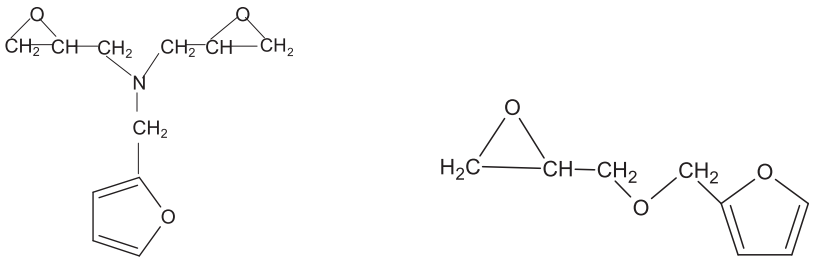

a b

Scheme 1. Structures of (a) DGFA and (b) FGE.

cured FGE is higher than its T_g. It means that load bearing ability of the material has to be drastically reduced in the course of crack elimination.

In consideration of complementarity of structure and properties between DGFA and FGE, blends of DGFA and FGE might be able to possess balanced performance. Accordingly, the present work is focused on characterization of thermal reversibility and healing efficiency of blended DGFA and FGE, and the influence of DGFA/FGE ratio as well. It is hoped that thermal remendability and mechanical properties of the new epoxy can be optimized as a result, and the family of epoxy that has been extensively used in many applications [9,10] can be expanded.

2. Experimental

2.1. Materials

The epoxy resins, DGFA and FGE, were synthesized in the authors' lab following the procedures described elsewhere [7,8]. The curing agents, methylhexahydrophthalic anhydride (MHHPA) and *N*,*N*′ (4,4′-diphenylmethane) bismaleimide (DPMBMI), were supplied by Aldrich Chemical Co., USA, which were used as received.

2.2. Curing of DGFA/FGE blends

DPMBMI was dissolved in DGFA, or FGE, or DGFA/FGE under stirring at 90 °C for 10 min. Then, MHHPA was added to the above mixture, and stirred at 80 °C within 10 min. The resultant homogeneous compound was degassed, poured into a closed silicone rubber mold, and cured at 70 °C for 24 h. Table 1 lists the formulations of the blends, in which the molar ratio of epoxide and anhydride groups is fixed at 1:0.8 and that of furan and maleimide groups is 1:1. These conditions were selected to provide the cured DGFA/FGE blends with as much as possible DA bonds.

2.3. Characterization

Fourier transform infrared (FTIR) spectra were recorded with a Bruker EQUINOX55 Fourier transformation infrared spectrometer. Differential scanning calorimetry (DSC) was performed on a TA Instruments DSC Q10 using nitrogen purge and an empty aluminum pan as a reference. Dynamic mechanical analysis (DMA) was conducted on a TA Instruments DMA 2980 at a heating rate of 5 °C/min. Raman measurements were carried out using a Renishaw inVia (UK) spectrometer equipped with a Leica microscope. The Raman spectra were excited by a 785 nm laser line at a resolution of 1 cm^{-1}, and the laser was focused by a 20× objective to a spot size of ~10 μm.

Healing efficiency of the materials was evaluated following the method suggested by Nemat-Nasser et al. [11], i.e. double cleavage drilled compression (DCDC) tests. The design allows for controlled incremental crack growth so that the cracked specimen remains in one piece after the test, ensuring realignment of the fracture surfaces prior to healing. The DCDC specimen was a column of a rectangular cross-section (length $L = 50$ mm, width $w = 15$ mm, thickness $t = 8.9$ mm) with a circular hole (radius $R = 1.98$ mm) drilled through its center that is subjected to axial compression. Prior to the test, a blade was wedged into the central hole of the DCDC specimen to create pre-cracks 0.5 mm deep at the upper and lower crowns. Then, a restraining clamp was placed around the specimen (Fig. 1) and axial compression was applied. The lateral confinement offered by the clamp prevented the cracks from growing beyond a length, l ($l/R = 0.8$), from the crowns of the hole. Afterwards, the clamp was removed and the specimen was reloaded in compression with a SANS CMT 6000 universal tester at a crosshead rate of 0.2 mm/min to record the force, σ_{crit}, and crack length, l/R, of the subsequent fracture event. The test was paused at increments of 60 μm in crosshead displacement and, after an equilibration period of 10 s, the peak load over that period was recorded and a photo was taken for determining crack length. After the test, the specimen was healed by staying in a pre-heated oven at a temperature slightly lower than the glass temperature for 20 min (for disconnecting DA bonds) and then at 80 °C for 72 h (for reconnecting the disconnected furan and maleimide moieties). Finally, the healed specimen was tested again following the above procedure. Healing efficiency, η, was calculated from the ratio of critical stress required to propagate the crack to a given length in the healed material, σ_{crit}^{healed}, to the stress required to propagate the crack to the same length in the virgin material, σ_{crit}^{virgin}. It is worth noting that the healing efficiency was originally defined as the ratio of the fracture toughness of the healed specimen over the fracture toughness of the virgin specimen [12], which only depended on

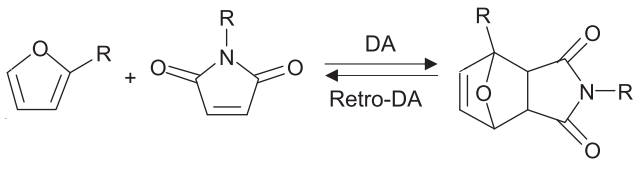

Scheme 2. DA and retro-DA reactions between furan and maleimide.

Table 1
Molar compositions of thermal remendable epoxy.

Sample ID	DGFA	FGE	DPMBMI	MHHPA
DF10	1	0	0.5	1.6
DF01	0	1	0.5	0.8
DF91	0.9	0.1	0.5	1.52
DF82	0.8	0.2	0.5	1.44
DF73	0.7	0.3	0.5	1.36
DF64	0.6	0.4	0.5	1.28

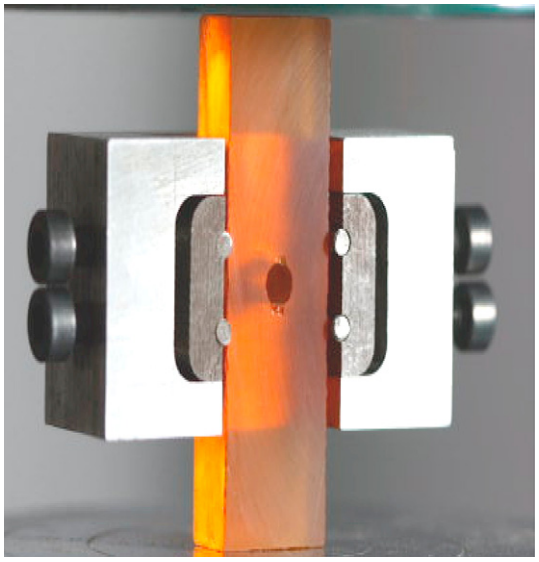

Fig. 1. A DCDC specimen with restraining clamp to create pre-crack. Small notches that were made by a blade in advance are visible at upper and lower crowns of the central hole.

material properties. The above simplified calculation based on the ratio of critical stresses, proposed by Nemat-Nasser et al. [11], is related to both material properties and geometry effects, and can be meaningful when the cracks in both the virgin and healed cases had nearly identical length. Accordingly, in order to obtain the healing efficiency in the present work, for a measured critical stress of the virgin specimen at a certain crack length, the corresponding critical stress of the healed specimen at the same crack length was estimated by interpolation from the fitted crack length dependence of the measured critical stress of the healed specimen.

3. Results and discussion

Since both DGFA and FGE carry the same functional groups (i.e. furan and epoxide), the DGFA/FGE blends can be cured by the same curing agents as DGFA or FGE alone: DPMBMI and MHHPA. The two hardeners are respectively responsible for establishing thermally reversible and irreversible bonds in the cured systems as mentioned in the Introduction. Fig. 2 shows FTIR spectra of the cured blends. It is seen that the peaks attributed to epoxide groups

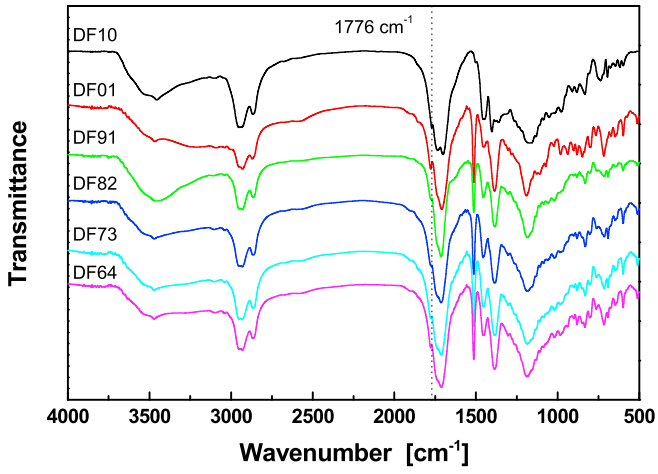

Fig. 2. FTIR spectra of cured DGFA/FGE blends. The sample IDs and compositions are shown in Table 1.

at 918 cm^{-1} (oxirane ring breathing) and 851 cm^{-1} (C–O–C) are absent, meaning that all epoxide groups must have reacted with anhydride groups of MHHPA to form epoxy networks. The evident peak of hydroxyl groups at around 3500 cm^{-1} also evidences the occurrence of the reaction. Meanwhile, the peak at about 1776 cm^{-1} manifests the existence of DA adduct from the reaction between furan and maleimide groups. It is known that in the cured blends the two types of desired macromolecular networks have been built up, regardless of blending ratio of DGFA and FGE resins.

Thermal reversibility of the cured blends is viewed by DSC in terms of repeated heating and cooling treatments. That is, the specimens were treated at 140 °C for 20 min to attain retro-DA samples and then at 80 °C for 72 h to attain DA samples reactions up to four times. The detailed steps are described in the caption of Fig. 3, which are the same as those used for verifying individual DGFA and FGE [7,8]. It is seen that an endothermic peak appears at around 120 °C on the curves of as-manufactured samples, which results from retro-DA reaction. As for rDA1, only a glass transition at around 120 °C is observed. It means that the treatment at 140 °C for 20 min has led to complete disconnection of DA bonds via retro-DA reaction. Subsequently, the rDA1 sample is allowed to reconnect the cleavage groups through DA reaction by rehabilitation at 80 °C for 72 h, so that an endothermic peak appears again on the DSC curve of DA1. The repeatable emergence of the endotherm evidences thermal reversibility of the DA bonds in the blends.

A careful survey of the data listed in Table 2 reveals that with a rise in the content of FGE in the blends, the enthalpy of retro-DA reaction increases. Clearly, an increased contribution from FGE should account for the variations because FGE contains more furan rings. Moreover, Table 2 also indicates that the peak temperature of retro-DA reaction decreases with the fraction of FGE. This should be attributed to the relatively less epoxide groups in FGE than DGFA, which reduces the restraint effect of epoxy networks.

It is interesting to note that for cured DGFA (i.e. DF10) the enthalpy of retro-DA reaction significantly decreases after the first cycle of heating and cooling, and this trend becomes less obvious in the subsequent tests. The phenomenon should be related to the increase in crosslinking density of the system as a result of heat treatment, which hinders recovery of DA bonds. However, when FGE is incorporated, the decrement becomes smaller. Consequently, recovery efficiency of the DA reaction is raised with increasing the concentration of FGE, which would certainly benefit the improvement of thermal remendability of the blends.

In addition to the DSC study under quiescent condition, DMA was also employed to examine thermal reversibility of the materials. The results are more closely related with mobility of the macromolecules. As illustrated in Fig. 4, storage moduli of as-manufactured samples drastically decrease with increasing temperature at around 110 °C and then level off. When temperature is further raised, the moduli drop again. In contrast, after retro-DA reaction at 140 °C for 20 min, the samples only show a single transition on the curves of storage moduli versus temperature, despite the fact that the room temperature storage moduli are reduced probably due to plasticization effect of the disconnected furan and maleimide moieties. Evidently, the two-stage variation in storage moduli of the as-manufactured samples reflects retro-DA reaction and glass transition, respectively. The retro-DA reaction happens below glass transition temperature of the materials, but there is still certain overlap between the two processes.

When the blends are heated above the glass transition temperature, all of DA bonds are broken. Thus, the storage moduli in the rubbery region are only related with the crosslinking density variations of epoxy networks. According to the equation of state for rubber elasticity, molecular weight between crosslinks of the cured epoxy, M_c, was calculated from [13]:

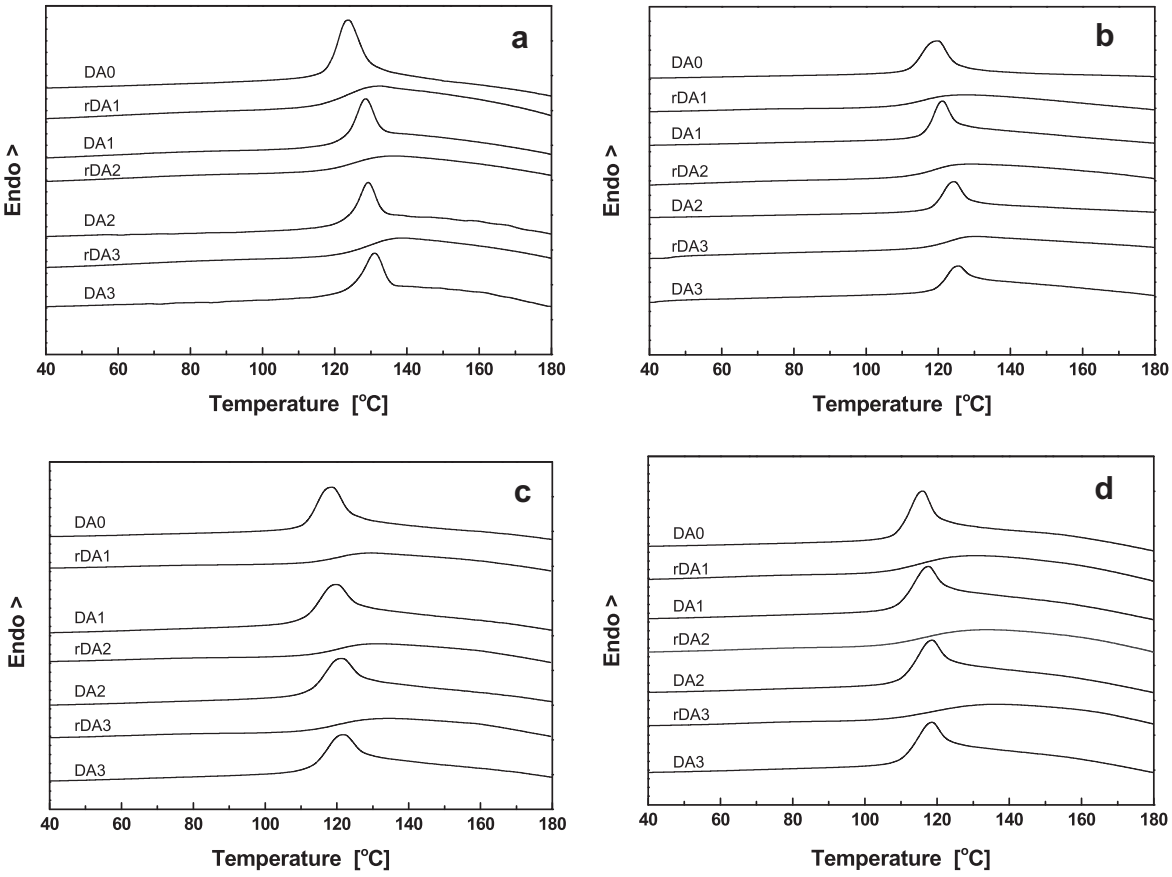

Fig. 3. DSC heating traces of the cured blends of DGFA and FGE (heating rate: 5 °C/min): (a) DF91, (b) DF82, (3) DF73, and (d) DF64. DA0: as-manufactured sample. rDA1: DA0 treated at 140 °C for 20 min, and then quenched to room temperature. DA1: rDA1 treated at 80 °C for 72 h, and then cooled inside oven by switching off electricity supply. rDA2: DA1 treated at 140 °C for 20 min, and then quenched to room temperature. DA2: rDA2 treated at 80 °C for 72 h, and then cooled inside the oven by switching off electricity supply. rDA3: DA2 treated at 140 °C for 20 min, and then quenched to room temperature. DA3: rDA3 treated at 80 °C for 72 h, and then cooled inside the oven by switching off electricity supply.

$$E' = 3\frac{\rho}{M_c}RT\left(1-\frac{2}{\varphi}\right) \quad (1)$$

where E' stands for storage modulus at rubbery plateau zone, ρ density, R gas constant, T absolute temperature, and φ functionality of epoxy, respectively. The plots in Fig. 5 demonstrate that after the retro-DA reaction, M_c is lowered in all the materials. In other words, the crosslink density of epoxy networks is increased accordingly. The results support the above analysis of reduced enthalpy of retro-DA reaction after cyclic heating and cooling (Table 2), and also explain higher T_g of the specimens after retro-DA reaction in comparison to the as-manufactured specimens (Figs. 4 and 5).

With respect to the effect of blending with FGE, the higher content of FGE, the higher M_c, either before or after retro-DA reaction. This implies that the thermal reversible DA bonds in the blends are more mobile in the case of high FGE fraction due to the surrounding looser epoxy networks.

To assess thermal remendability of the blends, double cleavage drilled compression (DCDC) tests were made (see Experimental). Typical crack length dependences of stress of virgin and healed cracked DF10 specimens are shown in Fig. 6. Tables 3 and 4 list healing efficiencies of DF10 and DF01 measured at different crack lengths, and the average healing efficiencies as well. Owing to the higher furan fraction in DF01

Table 2
Thermal reversibility of DA reaction in the cured blends of DGFA and FGE.

Blends	DF10[a]				DF01[a]			DF91			DF82			DF73			DF64	
Treatment[b]	T_p[c] (°C)	ΔH[d] (J/g)	R[e] (%)	T_p (°C)	ΔH (J/g)	R (%)	T_p (°C)	ΔH (J/g)	R (%)	T_p (°C)	ΔH (J/g)	R (%)	T_p (°C)	ΔH (J/g)	R (%)	T_p (°C)	ΔH (J/g)	R (%)
DA0	126.2	122.9	–	113.0	176.4	–	124.0	126.6	–	120.0	132.1	–	118.5	136.5	–	116.0	140.4	–
DA1	131.6	94.7	77.1	114.1	175.2	99.3	128.0	100.5	79.4	121.5	113.5	85.9	119.5	118.5	86.8	117.5	122.1	87.0
DA2	133.7	92.6	75.3	114.6	174.8	99.1	129.0	98.7	78.0	124.5	108.4	82.1	121.5	111.2	81.5	118.0	120.0	85.5
DA3	136.5	90.0	73.3	114.6	174.0	98.6	131.0	96.0	75.8	125.5	105.9	80.2	122.0	110.1	80.7	119.0	116.2	82.8

[a] The data of DF10 and DF01 are quoted from ref.[7,8].
[b] Treatment: The symbols (DA0–DA3) stand for cyclic heating and cooling treatments applied to the specimens (refer to Fig. 3).
[c] T_p: peak temperature for retro-DA reaction.
[d] ΔH: enthalpy of the endothermic peak due to retro-DA reaction.
[e] R: recovery efficiency of DA reaction, calculated from the enthalpy ratio of the retro-DA of DAi (i = 1, 2 and 3) to the retro-DA of DA0.

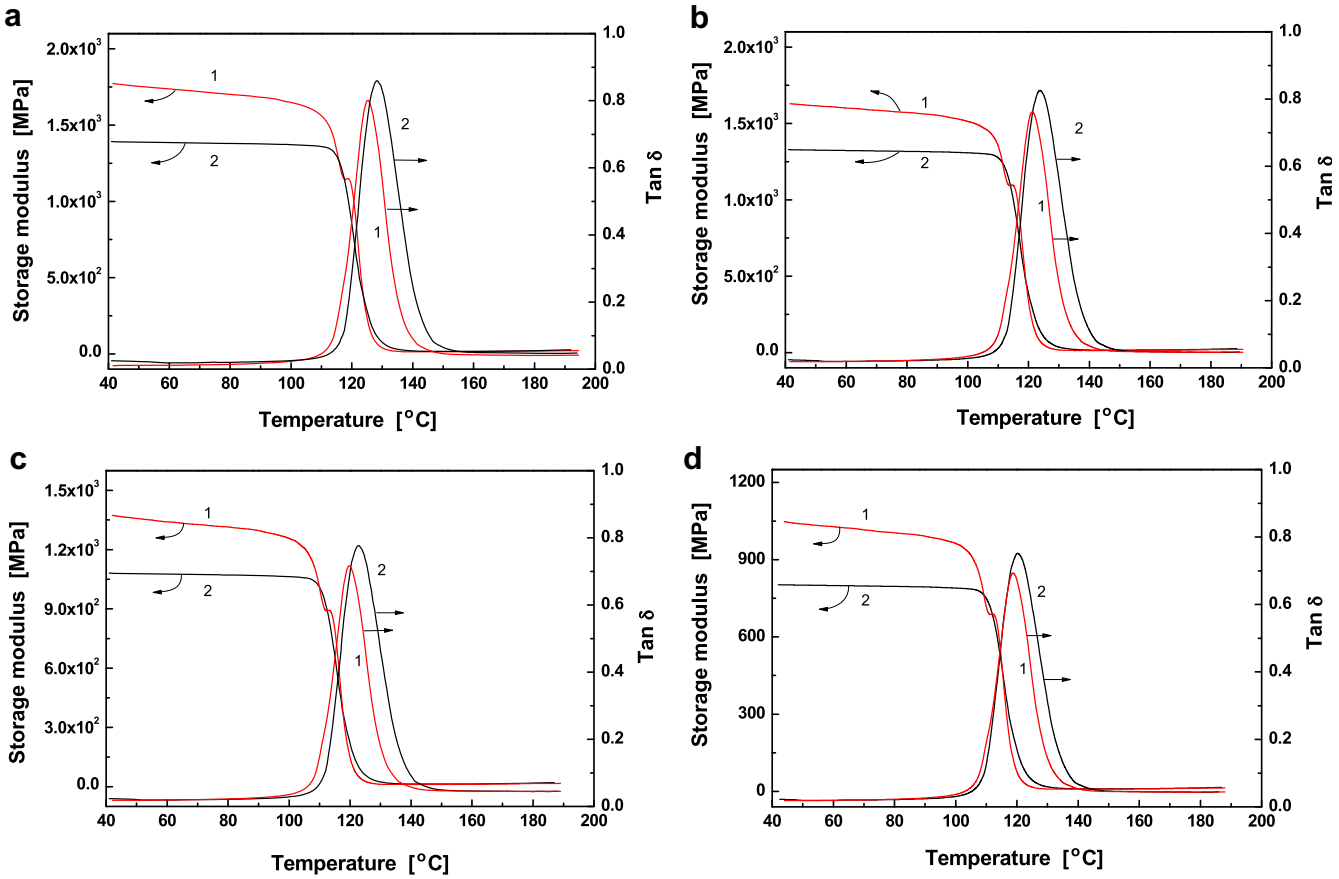

Fig. 4. DMA spectra of the cured blends of DGFA and FGE: (a) DF91, (b) DF82, (3) DF73, and (d) DF64. Curve 1: as-manufactured sample; curve 2: as-manufactured sample treated at 140 °C for 20 min, and then quenched to room temperature.

than in DF10, the former exhibits remarkably higher healing efficiency as expected.

Healing efficiencies of DF91, DF82, DF73 and DF64 are given in Tables 5–8. The temperatures for obtaining retro-DA specimens were so selected that they are near the peak retro-DA temperature and below T_g. This would guarantee disconnection of the DA bonds as much as possible, while the entire process of crack removal is conducted in glass state, which is critical for keeping profiles of the materials in practical applications. The results show that the addition of FGE greatly increases remendability of the system. The average healing efficiency is improved from 65.9% (for DF10) to 81.1% (for DF64). The increased amount of DA bonds in the blends must have taken effect.

Surface Raman spectra of the specimens were collected. The results of DF91 are shown in Fig. 7 as the representative. The peak at 1618 cm^{-1} is attributed to stretching mode of benzene, while those at 1385 and 1448 cm^{-1} are interpreted as breathing of furan rings. The peaks at 794 and 837 cm^{-1} are due to ether bonds resulting from ring opening of epoxide groups. Therefore, when area of the peak at 1618 cm^{-1} acts as the reference, concentration of furan

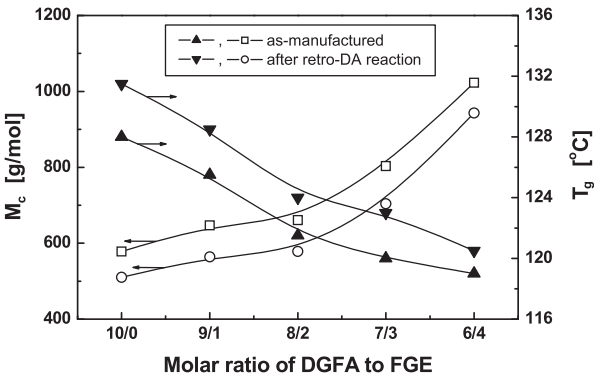

Fig. 5. Molecular weight between crosslinks of the cured epoxy, M_c, and glass transition temperature, T_g, of the cured blends of DGFA and FGE as a function of molar ratio of DGFA to FGE. The data are derived from the corresponding DMA spectra, and M_c values are estimated using storage moduli at 160 °C according to Eq. (1).

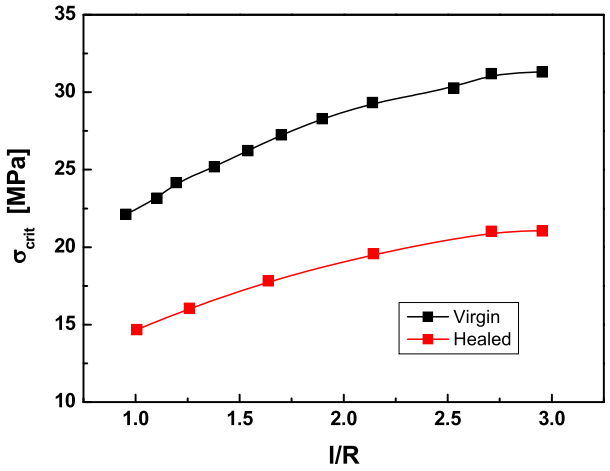

Fig. 6. Typical critical stress, σ_{crit}, versus crack length, l/R, of DF10 specimens.

Table 3
Healing efficiency of DF10 specimen.

Crack length	$l/R = 1.00$		$l/R = 1.26$		$l/R = 2.14$		η_{avg} (%)
	σ_{crit} (MPa)	η (%)	σ_{crit} (MPa)	η (%)	σ_{crit} (MPa)	η (%)	
Virgin[a]	22.5	–	24.4	–	29.1	–	–
Healed[b]	14.7	65.0	16.1	65.8	19.6	67.0	65.9

[a] Virgin: as-manufactured specimen.
[b] Healed: cracked virgin specimen was treated at 126 °C for 20 min, and then at 80 °C for 72 h. The treatment temperature 126 °C is close to the peak retro-DA temperature (Table 2) and lower than T_g (Fig. 5).

Table 4
Healing efficiency of DF01 specimen.

Crack length	$l/R = 1.11$		$l/R = 1.72$		$l/R = 2.18$		η_{avg} (%)
	σ_{crit} (MPa)	η (%)	σ_{crit} (MPa)	η (%)	σ_{crit} (MPa)	η (%)	
Virgin[a]	8.51	–	9.94	–	10.68	–	–
Healed[b]	8.16	95.9	9.55	96.0	10.26	96.1	96.0

[a] Virgin: as-manufactured specimen.
[b] Healed: cracked virgin specimen was treated at 110 °C for 20 min, and then at 80 °C for 72 h. The treatment temperature 110 °C is close to the peak retro-DA temperature (Table 2) and higher than T_g (93.5 °C, measured by DSC, refer to ref. [8]). Because the loss in modulus during glass transition of cured FGE is so severe that no complete DMA spectrum can be recorded, here we have to use the T_g determined by DSC.

Table 5
Healing efficiency of DF91 specimen.

Crack length	$l/R = 1.03$		$l/R = 1.65$		$l/R = 2.19$		η_{avg} (%)
	σ_{crit} (MPa)	η (%)	σ_{crit} (MPa)	η (%)	σ_{crit} (MPa)	η (%)	
Virgin[a]	21.2	–	27.1	–	27.4	–	–
Healed[b]	14.4	68.0	18.6	68.6	18.6	67.9	68.2

[a] Virgin: as-manufactured specimen.
[b] Healed: cracked virgin specimen was treated at 121 °C for 20 min, and then at 80 °C for 72 h. The treatment temperature 121 °C is close to the peak retro-DA temperature (Table 2) and lower than T_g (Fig. 5).

Table 6
Healing efficiency of DF82 specimen.

Crack length	$l/R = 1.00$		$l/R = 1.26$		$l/R = 2.14$		η_{avg} (%)
	σ_{crit} (MPa)	η (%)	σ_{crit} (MPa)	η (%)	σ_{crit} (MPa)	η (%)	
Virgin[a]	18.9	–	20.5	–	24.5	–	–
Healed[b]	13.94	73.8	15.21	74.2	18.13	74	74.0

[a] Virgin: as-manufactured specimen.
[b] Healed: cracked virgin specimen was treated at 117 °C for 20 min, and then at 80 °C for 72 h. The treatment temperature 117 °C is close to the peak retro-DA temperature (Table 2) and lower than T_g (Fig. 5).

Table 7
Healing efficiency of DF73 specimen.

Crack length	$l/R = 1.1$		$l/R = 1.53$		$l/R = 2.18$		η_{avg} (%)
	σ_{crit} (MPa)	η (%)	σ_{crit} (MPa)	η (%)	σ_{crit} (MPa)	η (%)	
Virgin[a]	16.52	–	18.67	–	20.9	–	–
Healed[b]	12.64	76.5	14.33	76.7	16.2	77.5	76.9

[a] Virgin: as-manufactured specimen.
[b] Healed: cracked virgin specimen was treated at 116 °C for 20 min, and then at 80 °C for 72 h. The treatment temperature 116 °C is close to the peak retro-DA temperature (Table 2) and lower than T_g (Fig. 5).

Table 8
Healing efficiency of DF64 specimen.

Crack length	$l/R = 0.89$		$l/R = 1.38$		$l/R = 2.02$		η_{avg} (%)
	σ_{crit} (MPa)	η (%)	σ_{crit} (MPa)	η (%)	σ_{crit} (MPa)	η (%)	
Virgin[a]	11.6	–	13.65	–	15.6	–	–
Healed[b]	9.4	81.0	11.1	81.3	12.61	81.0	81.1

[a] Virgin: as-manufactured specimen.
[b] Healed: cracked virgin specimen was treated at 114 °C for 20 min, and then at 80 °C for 72 h. The treatment temperature 114 °C is close to the peak retro-DA temperature (Table 2) and lower than T_g (Fig. 5).

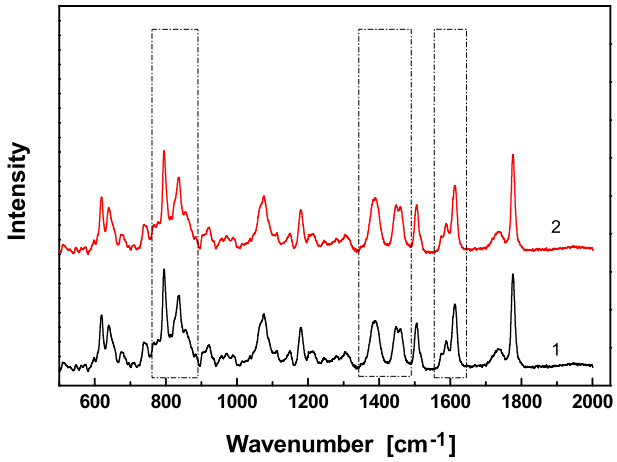

Fig. 7. Raman spectra of DF91 collected from (1) the as-manufactured surface and (2) the fractured surface.

rings can be characterized by areas of the peak at 1385 and 1448 cm^{-1}, and that of the crosslinked bonds of epoxy can be described by areas of the peaks at 794 and 837 cm^{-1}. Fig. 8 indicates that the content of furan groups characterized by peak area ratio, $A_{furan}/A_{benzene}$, is indeed increased with a rise in the content of FGE. Therefore, the blends with higher dosage of FGE contain higher concentration of DA bonds and possess higher healing efficiency.

Fig. 8 also reveals that the contents of furan groups on fractured surfaces are higher than those on as-manufactured surfaces. Comparatively, the contents of crosslinked bonds of epoxy are almost the same on either fractured or as-manufactured surfaces. Because the furan and epoxide groups are homogeneously distributed in the materials on molecular scale, the higher contents

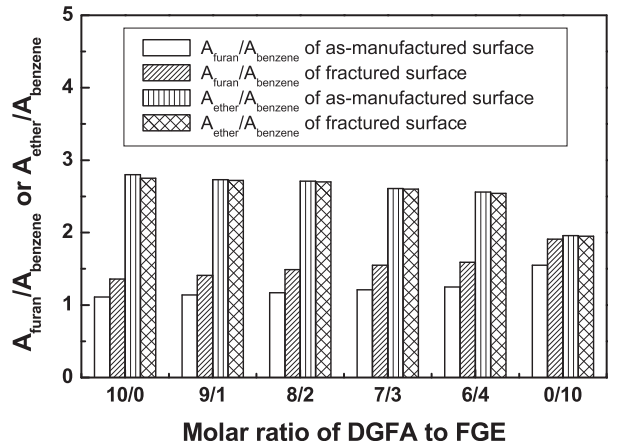

Fig. 8. Characteristic surface Raman peak area ratios of the cured blends of DGFA and FGE as a function of molar ratio of DGFA to FGE.

Table 9
Mechanical properties of the cured blends of DGFA and FGE.

Properties	Bisphenol-A epoxy cured by MHHPA [14]	DF10	DF01	DF91	DF82	DF73	DF64
Young's modulus (GPa)	1.8	2.5	0.9	2.3	2.1	1.77	1.35
Tensile strength (MPa)	65	53	19	48.2	44.5	37.6	28.6
Elongation at break (%)	–	1.5	0.5	1.4	1.5	1.6	1.4
Flexural modulus (GPa)	2.6	4.6	1.6	4.2	3.8	3.3	2.4
Flexural strength (MPa)	128	110	32	100	92.4	78	58

of furan groups on fractured surfaces imply that cracks have propagated preferentially along DA bonds. This agrees with the conclusion by Chen et al. [4] that the energy to break DA adducts is much lower than that to break all the other covalent bonds. Our estimation based on quantum chemistry also indicates that the length of the DA bond is 1.59 Å, which is 0.05 Å longer than conventional C–C bond length, so that the energy of DA bond has to be reduced. Owing to this feature of DA bonds, the polymers studied in the present work exhibit healing efficiency much higher than the estimation based on the true concentration of furan groups. For DF64, for example, the amount of furan groups only makes up 40% of the total amount of functional groups (i.e. the sum of furan and epoxide groups), but the healing efficiency is 81.1%.

Besides crack remendability, mechanical performance of the blends should also be characterized. As shown in Table 9, although tensile and flexural properties of the blends decrease with increasing the concentration of FGE due to its lower crosslinking density, most blends have comparable load bearing capability like the cured commercial bisphenol-A epoxy. The moduli of DF91–DF73 are slightly higher than that of bisphenol-A epoxy, while their strengths are moderately lower. On the whole, the properties data are satisfactory and the blends might replace traditional epoxy resin in future applications.

4. Conclusions

Owing to the structural complementarity of the blending components, balanced thermal remendability and mechanical properties are observed in the cured blends of DGFA and FGE resins. On one hand, concentration of DA bonds is higher than that in DGFA due to the incorporation of FGE that contains more furan groups, so that the fraction of intermonomer linkages that can be disconnected and reconnected upon specific heat treatment is increased accordingly. Obviously improved crack healing efficiency measured by DCDC tests is observed. On the other hand, concentration of crosslinked bonds of epoxy is also higher than that in FGE as a result of addition of DGFA. Consequently, the crosslinked epoxy networks not only provide the blends with acceptable load bearing ability but also enable elimination of cracks below T_g, which are important for practical applications.

Acknowledgements

The authors thank the support of the Natural Science Foundation of China (Grants: 50573093, U0634001 and 20874117). The valuable discussion with Professor Cunyuan Zhao on DA bonds is greatly appreciated.

References

[1] Yuan YC, Yin T, Rong MZ, Zhang MQ. Express Polymer Lett 2008;2:238.
[2] Bergman DS, Wudl F. J Mater Chem 2008;18:41.
[3] Chen XX, Dam MA, Ono K, Mal A, Shen H, Nutt SR, et al. Science 2002;295:1698.
[4] Chen XX, Wudl F, Mal AK, Shen HB, Nutt SR. Macromolecules 2003;36:1802.
[5] Liu YL, Hsieh CY. J Polym Sci Polym Chem 2006;44:905.
[6] Liu YL, Chen YW. Macromol Chem Phys 2007;208:224.
[7] Tian Q, Yuan YC, Rong MZ, Zhang MQ. J Mater Chem 2009;19:1289.
[8] Tian Q, Rong MZ, Zhang MQ, Yuan YC. Polym Int. (in press).
[9] Lin HT, Lin CH, Hu YM, Su WC. Polymer 2009;50:5685.
[10] Morell M, Ramis X, Ferrando F, Yu Y, Serra A. Polymer 2009;50:5374.
[11] Plaisted TA, Nemat-Nasser S. Acta Mater 2007;55:5684.
[12] Brown EN, Sottos NR, White SR. Exp Mech 2002;42:372.
[13] He MJ. Polymer physics. Shanghai: Press of Fudan University; 1990. p. 334 [in Chinese].
[14] Tao ZQ, Yang SY, Ge ZY, Chen JS, Fan L. Eur Polym J 2007;43:550.